Available online at www.sciencedirect.com
SCIENCE DIRECT®
Journal of Nuclear Materials 348 (2006) 94–101
journal of nuclear materials
www.elsevier.com/locate/jnucmat

Determination of elastic modulus and residual stress of plasma-sprayed tungsten coating on steel substrate

J.H. You *, T. Höschen, S. Lindig

Max-Planck-Institut für Plasmaphysik, EURATOM Association, Boltzmann Street 2, 85748 Garching, Germany

Received 8 April 2005; accepted 8 September 2005

Abstract

Plasma-sprayed tungsten, which is a candidate material for the first wall armour, shows a porous, heterogeneous microstructure. Due to its characteristic morphology, the properties are significantly different from those of its dense bulk material. Measurements of the elastic modulus of this coating have not been reported in the literature. In this work Young's modulus of highly porous plasma-sprayed tungsten coatings deposited on steel (F82H) substrates was measured. For the fabrication of the coating system the vacuum plasma-spray process was applied. Measurements were performed by means of three-point and four-point bending tests. The obtained modulus values ranged from 53 to 57 GPa. These values could be confirmed by the test result of a detached coating strip, which was 54 GPa. The applied methods produced consistent results regardless of testing configurations and specimen sizes. The errors were less than 1%. Residual stress of the coating was also estimated.

1. Introduction

Tungsten is one of the candidate materials for plasma-facing armour of the first wall components in a fusion reactor. Plasma-sprayed coatings usually show a porous, heterogeneous microstructure. Their typical porosity amounts to 20%. The pores have fairly irregular shapes and a wide size distribution often exhibiting conjoining neighbouring pores. Due to such characteristic morphology, properties of the plasma-sprayed coatings are significantly different from those of the dense bulk counterparts.

In general, component design and structural analysis are based on a macroscopic length scale. It means that the stress computation of the porous tungsten coating deposited on a large component requires materials data of homogenised (i.e., volume-averaged) properties which are also based on a macroscopic length scale. To author's knowledge, measurements of the homogenised elastic modulus of plasma-sprayed tungsten coating have not yet been reported in the literature. A rigorous analytical estimation, e.g., Eshelby–Mori–Tanaka method, is in general not viable whereas the finite element method may be applied to simulate the elastic deformation of such coatings from which the

* Corresponding author. Tel.: +49 89 3299 1373; fax: +49 89 3299 1212.
E-mail address: jeong-ha.you@ipp.mpg.de (J.H. You).

0022-3115/$ - see front matter © 2005 Elsevier B.V. All rights reserved.
doi:10.1016/j.jnucmat.2005.09.015

homogenised elastic modulus could be deduced. In this case, three-dimensional mapping of the microstructure into a mesh model will be the major technical difficulty.

The aim of this work is to measure Young's modulus of a plasma-sprayed thick porous tungsten coating deposited on a steel (F82H) substrate. There are various non-destructive test methods by which Young's modulus could be measured. These are for example vibrating reed, inverted torsion pendulum, ultrasonic pulse-echo and bending test, etc. [1]. In this work, the bending test method was applied which provides a possibility to perform a series of various mechanical characterisations consecutively without substantial modification of the test configuration.

The measured size of the pores in the tungsten coating ranged between 10 and 100 μm. Due to the presence of such relatively large pores, the specimen should not be so much down sized that the homogenisation assumption loses its validity. The dimension of a specimen (for example, thickness) should be sufficiently larger than the characteristic length scale of the pores so that the local morphology does not affect the measurement. In this work, bending experiments were performed for three different specimen sizes to explore the possible effect of specimen size.

Thermal spraying usually generates residual stress in the coating system. If the magnitude of residual stress is considerably large, the elastic limit of the materials can be readily exceeded even during processing or during subsequent testing. Hence, it is important to ensure that bending tests for elastic modulus measurements are conducted without any plastic yield. To this end, information on the stress state in the coating system is needed to control the maximum stress. The estimation of residual stress is another topic treated in this work. It was assumed that the presence of residual stress itself would not affect the system stiffness within the elastic regime.

2. Testing scheme and model systems

The tungsten coating/steel (F82H) substrate system used for the experiments was originally developed as an actively cooled first wall panel of a fusion reactor. F82H is a reduced-activation martensitic steel (Fe–8Cr–2W–0.2V–0.04Ta–0.1C). Tungsten coating was deposited using the vacuum plasma-spray (VPS) technique (Fig. 1) by the PLANSEE company. The fabricated component had a flat, rectangular shape with two material layers. The tungsten coating thickness, which was not ideally uniform along the width, ranged between 1.65 and 1.80 mm. The component showed actually no residual curvature due to the stiffness of thick substrate (7.35 mm). A rectangular cooling channel made of a stainless steel with a cross-section of $52 \times 6\ \text{mm}^2$ was welded to the substrate bottom before the spray process. This component panel was actively cooled also during the thermal spray process in order to reduce the residual stress. Cooling water with a temperature of 20 °C and flow rate of 10 l/min was used [2]. The basic physical properties and heat flux fatigue test of this coating system were reported in the literature [3].

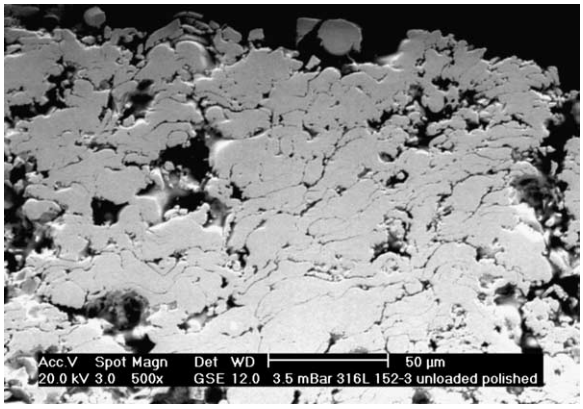

Fig. 1. Porous microstructure of a plasma-sprayed tungsten coating (SEM image).

After the thermal deposition, the component was machined to remove the cooling channel and to reduce the substrate thickness. After thinning and fine polishing, the final substrate thickness was reduced to 1.35 mm (Fig. 2). The thinning of the substrate was necessary in order to improve the sensitivity of the coating response and to avoid transverse shear deformation. Further machining was made to trim off the rough edges. The coating surface was also precisely polished in order to obtain a uniform coating thickness throughout the specimen. The final coating thickness was 1.62 mm. The dimensional error of the thickness was less than 1%. A notable feature of the thinned specimen was the remarkable residual curvature caused by the residual stress. The measured radius of curvature was (1.70 ± 0.02) m.

In the current experiment, both three-point and four-point bending tests were made. In an ideal case, the measured modulus would be independent

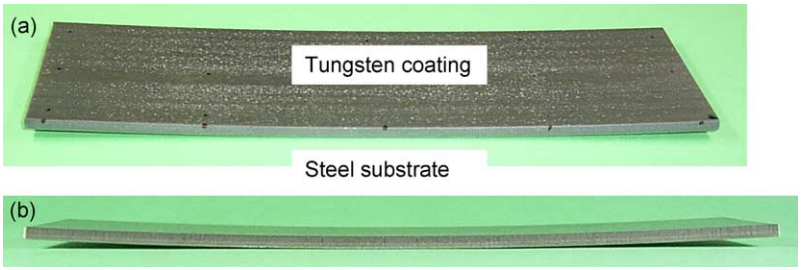

Fig. 2. A typical specimen form prepared for bending tests. Notable curvature (convex downward) caused by residual stress is observable: (a) birds view, (b) side view.

of the applied testing configurations. The schematic testing configuration for the four-point bending case is illustrated in Fig. 3. The coating was loaded only in compression to avoid local cracking. In case of the four-point bending test, displacements were measured by two different strain sensors: contact extensometer and laser-speckle interferometer. The former measures the total displacement at the maximum deflection position (position B) whereas the latter detects the relative displacement between the specimen centre (position B) and the loading point (position A).

The contact extensometer had a standard setup with a maximum arm travel range of 2 mm. It fulfils the European norm requirements prEN 10002 (linearity error 0.05%, display error 0.2%, indication error 0.5 μm). The frame of the extensometer was fixed on a stiff support next to the bending specimen. The contact arm was set to touch the specimen at the middle of the specimen. The lower supports were assumed to be rigid. The laser-speckle interferometer simultaneously measures the vertical displacement of two lateral surface positions by means of two laser illumination spots. The vertical displacement of the upper loading supports was detected by the upper laser spot using a marker bar mounted on them. The lower laser spot detected the vertical displacement at the middle of the specimen. The obtained values could be referred to the position of outer supports. The accuracy error of the laser interferometer device was below 1% of the measured values.

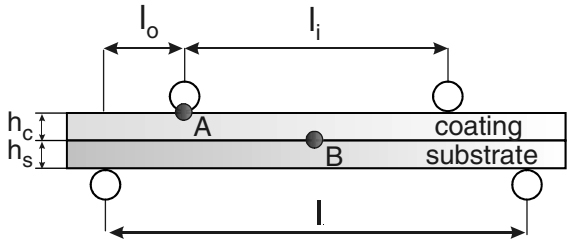

Fig. 3. Standard setting for four-point bending tests used for the experiment. The parameters defining setting measures are also indicated.

Young's modulus was determined from the measured force–deflection curves using two different approaches. At first, Young's modulus of the coating was directly extracted by means of rigorous mathematical relations derived for bending mechanics of a bi-material beam. Alternatively, the coating modulus was obtained by the simple rule of mixture in which the total modulus of the specimen was multiplied by the volume fraction of the coating layer. Theoretically, these two methods should yield identical results.

Test specimens with three different sizes were prepared (Table 1). Only the dimension of the planar face was varied. Finally, the coating layer was detached from the substrate and tested again by conventional bending. All tests were performed only in the linear elastic regime. Preliminary calibration tests were made using a thin steel plate with a known elastic property. The testing conditions are listed in Table 2. Each test case was repeated five times.

For comparison, the stress measurement was carried out on the coating surface using an X-ray diffractometer (device: PTS 3003 Seifert, Germany). The residual stress was measured using the standard $\sin^2(\Psi)$-method in which the lattice strain of a

Table 1
Geometry of three specimen sizes used for the bending tests

Geometry	Dimension (mm^3)
Small specimen	$12 \times 90 \times 2.97$
Medium specimen	$25 \times 90 \times 2.97$
Large specimen	$50 \times 180 \times 2.97$

Table 2
Bending test conditions and measured results (thickness, setting parameters, typical loads, typical deflections)

Test parameters	Small size	Medium size	Large size
h_c, h_s (mm)	1.62, 1.35	1.62, 1.35	1.62, 1.35
l (three-point)	70	70	160
l,l_o, l_i (four-point)	70, 15, 40	70, 15, 40	160, 45, 70
P_3 (N)	250	501	230
P_4 (N)	250	501	300, 330
w_3 (μm)	635	644	1802
w_4 (μm)	364	364	1670
$w_{4,r}$ (μm)	136	121	393

Zero point corrections are not included in the force and displacement values. Each deflection value is the average of five test results.

stressed sample is measured from the shift of the angular position of diffraction peaks. The in-plane stress component (parallel direction to the surface) was measured for a range of in-plane hoop orientations φ on the surface by rotating the sample (0–90°). The used Bragg angle was 131.16° and the selected peak was from the (3 2 1) lattice planes. The spot size of the incident beam on the surface was around 4 mm in diameter. The mass absorption coefficient of the used Cu Kα radiation in tungsten is very large (171 cm^2/g). Therefore, the obtained diffraction peaks stemmed mainly from the first deposition layer (single splat thickness) of the tungsten coating. For calculation of the stress we used Young's modulus and the Poisson ratio of dense tungsten.

3. Theoretical background

3.1. Estimation of residual stress

The total stress in a specimen under loading is the sum of residual stress and applied bending stress. It is an important prerequisite that the total stress is limited within the linear elastic regime. If residual stress is sufficiently strong, then local plastic flow or other inelastic processes can occur already from the beginning of loading. Hence, it is desirable to estimate residual stress in order to set adequate testing loads.

In this work, the residual stress of the tungsten coating/steel substrate system was calculated using the theoretical method developed by Tsui and Clyne [7]. This model was based on a set of conventional equilibrium equations of force and moment formulated for each successive incremental coating step. They assumed that a quasi-stationary thermal equilibrium is established between heat inflow and heat removal by cooling. Detailed expressions for final residual stresses are found in the literature. For calculations, one needs to know the elastic constants of both materials prior to estimation. Since the modulus of the coating was unknown in our case, it was at first roughly measured with a very small load. The tentative value was 55 GPa. The elastic modulus of the steel was 210 GPa. The assumed Poisson ratio of the coating and the steel was 0.1 and 0.3, respectively.

Quenching stress and mismatch stress are two major contributions to the residual stress [4–7]. The so-called quenching stress is generated by rapid cooling of hot-sprayed molten splats striking the substrate whereas the mismatch stress sets up due to the mismatch of thermal contraction during the final cooling (cooling from the steady state deposition temperature to ambient temperature). The theoretical method of Tsui and Clyne requires the information about the quenching stress as well as the temperature drop upon final cooling. Unfortunately, both of these quantities were not known for tungsten.

The theoretical value of the quenching stress is proportional to Young's modulus, the thermal expansion coefficient (CTE) and the temperature change during the quenching. Kuroda and Clyne measured the quenching stress of several pure metals, which ranged from 25 to 55 MPa in case of the cold substrate. They showed that the measured quenching stresses were significantly smaller than the theoretical maximum values due to the strong stress relaxation [4]. It was also found that the actual quenching stress was essentially affected by the substrate temperature normalised by the melting point of the coating materials.

In this work, a parametric assessment of the residual stress was made assuming four different quenching stress values. The considered quenching stress values were 35, 45, 55 and 65 MPa. On the other hand, the temperature drop upon final cooling was calculated for the assumed quenching stress values utilising the measured residual curvature of the specimen. Using the model of Tsui and Clyne, the temperature drop for a given quenching stress was calculated by iteration in which the computed curvature was compared with the measured one. The iteration was continued by updating the temperature until the convergence was achieved. The full iteration loop was repeated for the four different quenching stress values, respectively.

3.2. Estimation of total stress

In the next step, the applied bending stress should be added to the residual stress to get the total stress. The analytical form of bending stress of a layered bi-material strip is easily found in the literature [8]. When a testing configuration is used as illustrated in Fig. 3 with a specimen deformed as in Fig. 2, the most critical position would be the bottom surface of the steel substrate, because both the applied bending stress and the residual stress attain the tensile maximum at this outermost position. The applied peak loads are listed in Table 2. The yield stress of the steel substrate was 500 MPa.

3.3. Estimation of elastic modulus of the coating

The elastic modulus was determined using the force–deflection equations formulated for three-point and four-point bending conditions. For the present specimen geometry, the bending stiffness S_b and tensile stiffness S_t are expressed by [8]:

$$S_b = \frac{1}{3}\left[E_c^* h_c^3 + E_s^*\left(h_t^3 - h_c^3\right)\right] - S_t\delta^2, \tag{1}$$

$$S_t = E_c^* h_c + E_s^* h_s \tag{2}$$

$$\text{with} \quad \delta = \frac{1}{2S_t}\left[E_c^* h_c^2 + E_s^*\left(h_t^2 - h_c^2\right)\right] \tag{3}$$

$$\text{and} \quad E_s^* = E_s/(1-\nu_s^2), \quad E_c^* = E_c/(1-\nu_c^2), \tag{4}$$

where h denotes thickness, b, width of the cross-section and z, coordinate along the loading axis. The subscripts c and s denote coating and substrate, respectively.

In the case of a three-point bending test, the total bending force P_3 and the maximum deflection w_3 are related by [9]

$$S_{b3} = \frac{P_3 l^3}{48 w_3}, \tag{5}$$

whereas the maximum deflection w_4 in a four-point bending test is linked to P_4 as follows [10,11]:

$$S_{b4} = \frac{P_4 l_o (3l^2 - 4l_o^2)}{48 w_4}. \tag{6}$$

Here, the subscripts 3 and 4 stand for three-point and four-point bending. The relative displacement between the positions A and B, $w_{4,r}$, is connected to P_4 by [8]

$$S_{b4} = \frac{P_4 l_i^2 l_o}{16 w_{4,r}}. \tag{7}$$

The setting parameters l, l_o and l_i are defined in Fig. 3. Having measured w_3, w_4 and $w_{4,r}$ for a set of prescribed P_3 and P_4 values, the elastic modulus of the coating layer E_c can be identified by solving the Eqs. (1)–(7).

On the other hand, the coating elastic modulus can also be determined directly from a bending force–deflection curve using the simple rule of mixture as follows:

$$E_c = \frac{P_3 l^3}{4 b h^3 w_3}\frac{h_c}{h_c + h_s}. \tag{8}$$

4. Results and discussion

In Fig. 4, the computed total residual stress profiles are shown for the whole range of the specimen thickness. For comparison, the experimental residual stress measured by X-ray diffraction is also plotted. The measured stress data are listed in Table 3 for seven different in-plane directions. Considering the coating microstructure, it was assumed that the global elastic property of the coating is essen-

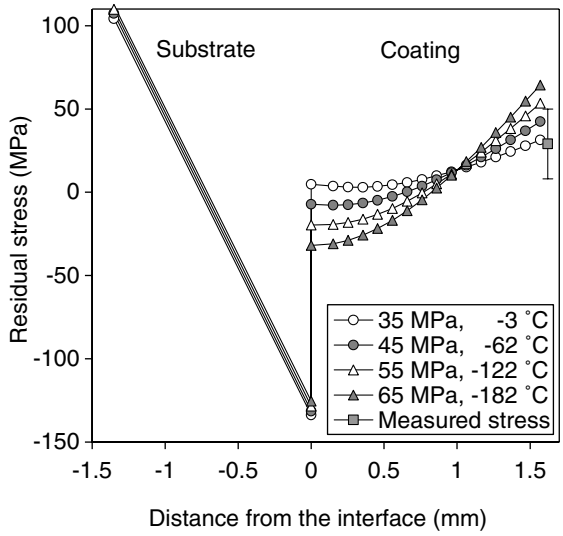

Fig. 4. Computed profiles of the total residual stress obtained for four different sets of the quenching stress and the temperature drop on final cooling. The stress values are plotted along the specimen thickness direction. The residual stresses are the sum of the quenching stress and the mismatch stress, which are not shown here. For comparison, the experimental stress value measured on the surface using X-ray diffractometry is also plotted with a error bar indicating standard deviation. The negative domain of the abscissa corresponds to the steel substrate while the positive part the plasma-sprayed coating.

Table 3
Surface stresses measured by X-ray diffractometer for different in-plane directions (φ angle)

φ Angle (°)	0	15	30	45	60	75	90	Average
Stress (MPa)	68	26	12	23	48	12	12	29 ± 21

The used Bragg angle was 131.16° and lattice planes were (321).

tially transversely isotropic, that is, isotropic in the in-plane directions (tangent to the surface). The measured in-plane stress values were averaged and compared with the theoretical stress values for the surface position as illustrated in Fig. 4. In the legend, the assumed quenching stress together with the corresponding temperature drop are given for each stress profile. The estimated temperature drop ranged from 3 to 182 K for the assumed quenching stress values from 35 to 65 MPa. The theoretical residual stress values agreed with the experimental result within an order of magnitude. The relatively large error scattering in the measured stress did not allow to determine the 'actual' quenching stress and temperature drop. For definite determination of the residual stress one of these unknown quantities should be further specified. Provided that the surface heat flux during the thermal spray is known, the temperature drop can be roughly assessed considering the Fourier heat conduction law and assuming a quasi-stationary thermal conduction. For example, in the case of a heat power of 7 kW, the 'average' temperature difference between the coating and the coolant is calculated to be 184 °C. This leads to the quenching stress value of 65 MPa for the given specimen curvature.

The values of the tungsten quenching stress considered here were comparable to those of molybdenum which ranged from 30 to 60 MPa for VPS coatings [4]. It is noted that both the refractory bcc metals possess similar mechanical and thermal properties.

The profiles of the total residual stress showed characteristic gradients in the coating. The shape of the specimen curvature being concave on the coating side (Fig. 2) clearly supported the predicted stress profiles. This feature might be an evidence for the essential contribution of the quenching stress to the final residual stress. In the case of a system with a thicker substrate the total residual stress becomes lower as the mismatch stress compensates for most of the quenching stress. For example, the current coating system with a substrate thickness of 7 mm would have residual stresses ranging from −6 (interface) to 10 (surface) MPa in the coating while the quenching stress at the surface would amount to 64 MPa.

A typical load–deflection curve measured from the three-point bending test is plotted in Fig. 5. Both loading and unloading steps are shown. It is seen that the unloading curve did not coincide with the loading line. The loading curve was resumed again upon subsequent reloading without change in the stiffness. This feature was observed in all testing results but could not be clearly understood. The measured deflections are listed in Table 2. Zero point corrections are not included in this data. Each deflection value is the average of five test results.

The final results of E_c are summarised in Table 4. The estimated E_c values are listed for the three specimen sizes and the four testing methods. The test result for the detached coating is also presented. The individual values are the average of the five repeated measurements. The errors related to the measurements and estimations were typically less than 1%. Good agreement could be achieved between the E_c values regardless of the test configurations and specimen sizes. The E_c values measured for the bi-material specimens could be confirmed by that of the detached coating strip. The obtained E_c values amounted roughly to 14% of the elastic modulus of dense tungsten (400 GPa). It is well known in the literature that a plasma-sprayed coating usually has a much smaller elastic modulus than its dense counterpart, typically less than 20–30% [11].

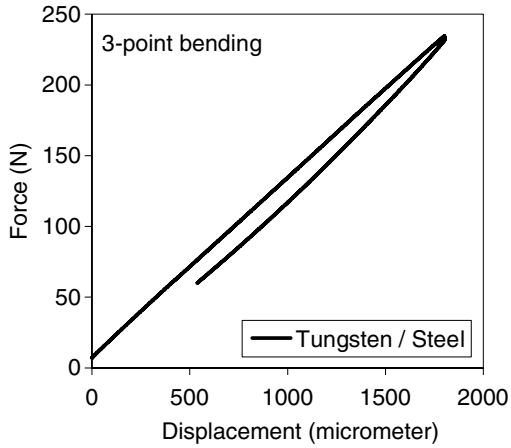

Fig. 5. A typical load–deflection curve of a three-point bending test for a layered bi-material coating system (length: 180 mm, width: 50 mm, l: 160 mm). Lines both for loading and unloading steps are shown. The initial loading curve was resumed upon reloading.

Table 4
Final results of Young's modulus estimation for the vacuum plasma-sprayed tungsten coating (modulus units in GPa)

Methods	Small size (compressive)	Medium size (compressive)	Large size (compressive)
Three-point bending	54.1 ± 0.5	57.5 ± 1.0	52.5 ± 0.7
Three-point bending (rule of mixture)	54.5 ± 0.4	55.6 ± 0.4	52.6 ± 0.3
Four-point bending (maximum deflection)	56.9 ± 0.2	57.1 ± 0.5	56.3 ± 0.6
Four-point bending (relative displacement)	53.5 ± 0.3	57.3 ± 0.5	57.0 ± 1.9
Four-point bending (detached coating)		54.1 ± 4.9	

This feature may be attributed to the porous microstructure and microcracks formed by poor bonding between splats. The presence of randomly shaped open-pores and their interconnection would contribute to the stiffness reduction as well.

It was thus demonstrated that both the three-point and four-point bending test methods could be properly applied. The size-irrelevance was also evident within the considered range of specimen dimensions.

5. Summary

Plasma-sprayed tungsten coating, which is a candidate material for the first wall armour, shows a porous, heterogeneous microstructure. Due to such a characteristic morphology, material properties of this coating are significantly different from those of the dense material. The aim of this work is to measure the elastic modulus of highly porous plasma-sprayed thick tungsten coating deposited on steel (F82H) substrate. To this end, a tungsten coating/steel substrate system was fabricated using the vacuum plasma-spray technique. After machining and polishing of the specimen the coating thickness was reduced to 1.62 mm and the substrate thickness to 1.35 mm.

Both three-point and four-point bending tests were applied for the measurement. In case of the four-point bending test, displacements were measured by two different strain sensors, that is, contact extensometer and laser speckle interferometer. To confine the maximum stress of the specimens within the elastic regime, the residual stress was estimated using the theoretical method developed by Tsui and Clyne. For the stress calculation, typical values of the quenching stress of pure metals were considered. The computed residual stress at the surface ranged from 31 to 64 MPa, which were comparable to the experimental stress measured by the X-ray diffractometer. The measured surface stress ranged from 12 to 68 MPa. The shape of the specimen curvature, which was concave on the coating side, supported the theoretical result.

Young's modulus was determined from the measured force–deflection curves using two different approaches. At first, Young's modulus of the coating was directly extracted by means of rigorous mathematical expressions. Alternatively, the coating modulus was obtained by the simple rule of mixture. Finally, the coating layer was detached from the substrate and tested again by bending. The experiments were performed for three different specimen sizes.

The measured modulus values ranged from 53 to 57 GPa. The modulus of the detached coating strip was 54 GPa. The applied methods produced consistent modulus values regardless of the testing configuration and specimen size. The testing errors and the dimensional error were less than 1%, respectively. The obtained modulus values correspond to 14% of the elastic modulus of dense tungsten (400 GPa). This behaviour was attributed to the porous microstructure and micro-cracks formed by poor bonding between splats.

References

[1] N. Meyendorf, in: H. Blumenauer (Ed.), Werkstoffprüfung, Deutscher Verlag für Grundstoffindustrie, Stuttgart, 1994, p. 306.
[2] PLANSEE, private communication.
[3] H. Greuner, H. Bolt, B. Böswirth, S. Lindig, W. Kühnlein, T. Huber, K. Sato, S. Suzuki, Vacuum Plasma-Sprayed Tungsten on EUROFER and 316L, in: Proceedings of the 23rd Symposium on Fusion Technology, Venice, Italy, September 20–24, 2004, Fus. Eng. Des., (2005) in press.
[4] S. Kuroda, T.W. Clyne, Thin Solid Films 200 (1991) 49.
[5] S.P. Timoshenko, J. Opt. Soc. Am. 11 (1925) 233.

[6] R. Elsing, O. Knotek, U. Balting, Surf. Coat. Technol. 43/44 (1990) 416.
[7] Y.C. Tsui, T.W. Clyne, Thin Solid Films 306 (1997) 23.
[8] J. Mencik, Mechanics of Components with Treated or Coated Surfaces, Kluwer Academic Publishers, Dordrecht, 1996.
[9] W. Schnell, D. Gross, W. HaugerTechnische Mechanik, vol. 2, Springer, Berlin, 1995.
[10] J.-M. Berthelot, Composite Materials, Springer, New York, 1999.
[11] A. Kucuk, C.C. Berndt, U. Senturk, R.S. Lima, C.R.C. Lima, Mater. Sci. Eng. A284 (2000) 29.